Available online at www.sciencedirect.com
ScienceDirect
Ceramics International 34 (2008) 1521–1525
CERAMICS INTERNATIONAL
www.elsevier.com/locate/ceramint

Effect of sintering temperature electrical properties of ZNR doped with Pr–Co–Cr–La

C.-W. Nahm

Department of Electrical Engineering, Dongeui University, Busan 614-714, South Korea

Received 20 February 2007; received in revised form 16 March 2007; accepted 24 April 2007
Available online 2 June 2007

Abstract

The microstructure, electrical properties, and dielectric characteristics of the ZNR (zinc oxide-based nonlinear resistors), which are composed of zinc oxide-based ceramics doped with Pr–Co–Cr–La, were investigated at different sintering temperatures (1240, 1245, 1250, 1255, 1260, and 1300 °C). The increase of sintering temperature led to more densified ceramics, whereas it decreased the nonlinear properties and breakdown voltage. The highest nonlinearity was obtained from 1240 °C, with 79.3 in nonlinear coefficient and 0.3 μA in leakage current. As the sintering temperature increased, the donor density increased from 0.90×10^{18} to $2.59 \times 10^{18}/cm^3$, and the barrier height decreased from 1.90 to 0.67 eV, and the dielectric dissipation factor increased from 0.0874 to 0.2839.

Keywords: A. Sintering; C. Electrical properties; D. ZnO; E. Nonlinear resistors

1. Introduction

Recent developments in electronic designs have tended toward smaller and higher density packaging of circuitry. This results in a greater susceptibility to surges. Once attacked by surge, electronic circuits can be destroyed in times as short as 0.1 μs. The designer of electronic equipment must be aware of, and be able to deal with, power surges in product design. The ZNR (zinc oxide-based nonlinear resistors) are attractive semiconducting ceramic devices made by sintering ZnO powder containing various minor additives, of nonlinear resistor-forming metal oxides such as Bi_2O_3, Pr_6O_{11}, V_2O_5, BaO, glass-frit, etc [1]. They are characterized by the nonlinear properties of voltage–current in the relation, $I = kV^{\alpha}$, where k is a constant and α is a nonlinear coefficient, which is an inherent parameter of the ZNR. In other words, they exhibit a voltage-dependent resistance, i.e. current increases sharply due to the decrease of impedance with increasing applied voltage. Moreover, they possess an excellent capability to withstanding surges. Hence, they have been extensively used in the field of circuit overvoltage protection, with applications ranging from a few volts in electronic circuits to million of volts in electric power systems [2].

Their electrical characteristics are related to a unit structure composed of zinc oxide grain – intergranular layer – zinc oxide grain in the bulk of the devices. A unit structure acts as if it has a semiconductor junction at the grain boundary. Since the nonlinear electrical behavior occurs at a boundary of each semiconducting zinc oxide grain, the ZNR can be considered a multi-junction device composed of many series and parallel connections of grain boundaries. The grain size distribution plays a major rule in electrical behavior.

Many researchers who are interested in the ZNR commonly wish to fabricate the ZNR with a higher nonlinearity. The majority of commercial ZNR are ZNR doped with Bi_2O_3 necessarily, which inherently induces nonlinear properties. Recently, the ZNR doped with Pr_6O_{11} have been studied in order to improve a few drawbacks [3] due to the high volatility and reactivity of Bi_2O_3 [4–14]. Nahm et al. reported that the ZNR doped with Pr–Co–Cr have highly nonlinear properties when rare-earth metal oxides, M_2O_3 (M = Er, Y, Dy, La) are added [11–14]. Furthermore, it is important to scrutinize the resistor characteristics according to manufacturing processes for individual additives to extend the application of ZNR doped with Pr_6O_{11} in various areas.

E-mail address: cwnahm@dongeui.ac.kr.

0272-8842/$34.00
doi:10.1016/j.ceramint.2007.04.014

The objective of this paper is to investigate the effect of sintering temperature on microstructure, electrical properties, and dielectric characteristics of ZNR doped with Pr–Co–Cr–La.

2. Experimental procedure

2.1. Sample preparation

Reagent-grade raw materials were prepared for ZNR with composition 97.0 mol% ZnO, 0.5 mol% Pr_6O_{11}, 1.0 mol% CoO, 0.5 mol% Cr_2O_3, 1.0 mol% La_2O_3. The chemicals were weighed and ball-milled with ZrO_2 balls and acetone in a polypropylene bottle for 24 h. The mixture was dried at 120 °C for 12 h and calcined at 750 °C for 2 h. The calcined mixture was pulverized using an agate mortar/pestle and after 2 wt% polyvinyl alcohol (PVA) binder addition, granulated by sieving 200-mesh screen to produce starting powder. The powders were uniaxially pressed into discs of 10 mm in diameter and 1.8 mm in thickness at a pressure of 80 MPa. The discs were sintered at six fixed sintering temperature 1240, 1245, 1250, 1255, 1260, and 1300 °C in air for 1 h. The size of the final samples was about 8 mm in diameter and 1.0 mm in thickness. Silver paste was coated on both faces of the samples and Ohmic contacts were formed by heating at 600 °C for 10 min. The size of electrodes was 5 mm in diameter.

2.2. Microstructure measurement

One side of the samples was lapped and ground with SiC paper and polished with 0.3 μm-Al_2O_3 powder to a mirror-like surface. The polished samples were thermally etched at 1100 °C for 30 min. The surface microstructure was examined by a scanning electron microscope (SEM, Hitachi S2400, Japan). The average grain size (d) was determined by the lineal intercept method, given by $d = 1.56L/MN$, where L is the random line length on the micrograph, M is the magnification of the micrograph, and N is the number of the grain boundaries intercepted by lines [15]. The crystalline phases were identified by X-ray diffractometry (XRD, Rigaku D/max 2100, Japan) with CuK_α radiation. The density (ρ) of sintered ceramics was measured by the Archimedes method.

2.3. Electrical and dielectric measurement

The voltage–current (V–I) characteristics of the ZNR were measured using a high voltage source-measure unit (Keithley 237). The breakdown voltage (V_B) was measured at a current density of 1.0 mA/cm^2 and the leakage current (I_L) was measured at 0.80 V_B. In addition, the nonlinear coefficient (α) was determined from $\alpha = (\log J_2 - \log J_1)/(\log E_2 - \log E_1)$, where $J_1 = 1.0$ mA/cm^2, $J_2 = 10$ mA/cm^2, and E_1 and E_2 are the electric fields corresponding to J_1 and J_2, respectively.

The capacitance–voltage (C–V) characteristics of the ZNR were measured at 1 kHz using an RLC meter (QuadTech 7600) and an electrometer (Keithley 617). The donor density (N_d) and the barrier height (ϕ_b) were determined by the equation $(1/C_b - 1/C_{bo})^2 = 2(\phi_b + V_{gb})/q\varepsilon N_d$ [16], where C_b is the capacitance per unit area of a grain boundary, C_{bo} is the value of C_b when $V_{gb} = 0$, V_{gb} is the applied voltage per grain boundary, q is the electronic charge, ε is the permittivity of ZnO ($\varepsilon = 8.5\varepsilon_o$). The density of interface states (N_t) at the grain boundary was determined by the equation $N_t = (2\varepsilon N_d \phi_b/q)^{1/2}$ [16] and the depletion layer width (t) of the either side at the grain boundaries was determined by the equation $N_d t = N_t$ [17].

The dielectric characteristics, such as the apparent dielectric constant (ε'_{APP}) and dissipation factor (tan δ) of the ZNR were measured in the range of 100 Hz–2 MHz using an RLC meter (QuadTech 7600).

3. Results and discussion

Fig. 1 shows the SEM micrographs of the ZNR ceramics at different sintering temperatures. It is well known that the microstructure of zinc oxide-based nonlinear resistor ceramics doped with Pr_6O_{11} consisted of only two phases [18]: zinc oxide grain (blackish) as primary phase and intergranular layer (whitish) as a secondary phase. The intergranular layers in resistor ceramics were Pr- and La-rich phases by XRD analysis, as shown in Fig. 2. As can be seen in the figure, three diffraction peaks were revealed in sintered ceramics, namely, zinc oxide

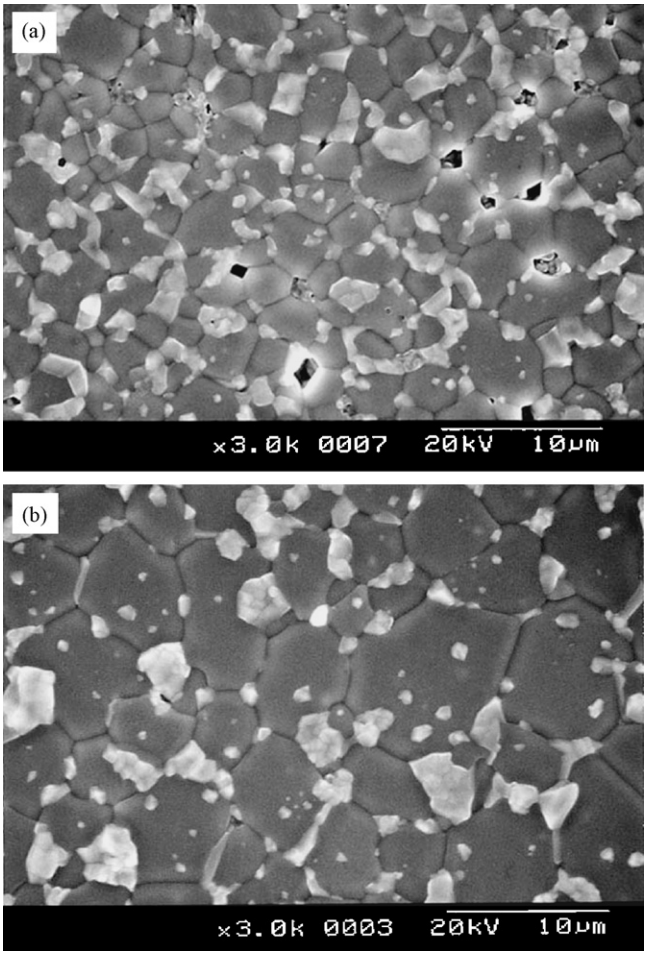

Fig. 1. Micrograph of the ZNR ceramics at different sintering temperatures: (a) 1240 °C and (b) 1300 °C.

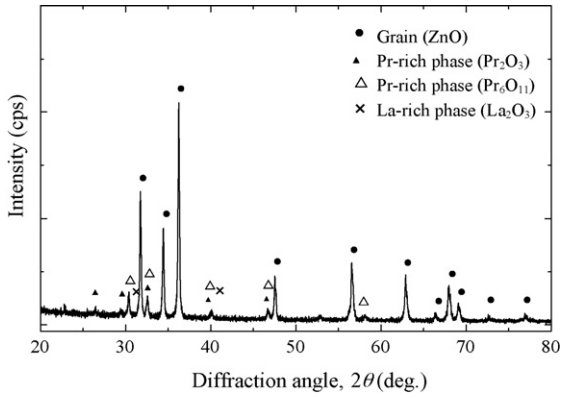

Fig. 2. XRD pattern of the ZNR ceramics doped with Pr–Co–Cr–La.

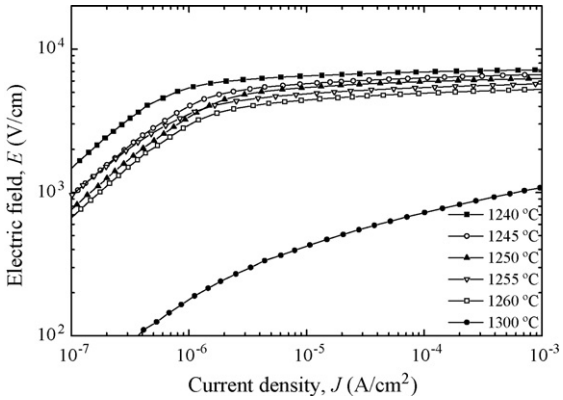

Fig. 4. *E–J* characteristics of the ZNR at different sintering temperatures.

grains, Pr oxides, and La_2O_3. It was found from EDX that these coexist at the grain boundaries and the nodal points as if they were a single phase. It is believed that this is attributed to the segregation of La toward grain boundaries due to the difference of ionic radius. It was observed by SEM that as the sintering temperature increased, the intergranular layer enlarged in size such as growing zinc oxide. These microstructures are not greatly different with resistor ceramics doped with Er, Y, and Dy, as reported previously [11–13].

Fig. 3 shows the average grain size (d) and sintered density (ρ) as a function of sintering temperatures. As the sintering temperature increased, the sintered density increased from 5.50 to 5.77 g/cm^3 and the average grain size increased from 4.2 to 7.9 μm. It can be seen that these ceramics show higher sintered density though the sintering temperature is low for the same composition ratio, compared with ceramics doped with Er, Y, and Dy possessing 5.58, 5.34, 5.43 g/cm^3, respectively, when it was sintered at 1350 °C [11–13]. The average grain size directly affects the breakdown voltage in the electrical properties.

Fig. 4 shows the *V–I* characteristics of the ZNR at different sintering temperatures. The conduction characteristics of the ZNR are remarkably divided into three regions: Ohmic region, so-call pre-breakdown region at low field; nonlinear region, so called breakdown region at intermediate field; and linear region, so-called upturn region. The sharper the knee of the curves between the Ohmic and nonlinear regions, the better the nonlinearity. The ZNR sintered in the range of 1240–1260 °C exhibited nearly similar shape of characteristic curves and will show high nonlinearity. However, it can forecast that for the ZNR sintered at 1300 °C the knee is less pronounced and the nonlinear properties will reduce.

Fig. 5 shows the breakdown voltage (V_B) and breakdown voltage per grain boundary (v_{gb}) as a function of sintering temperature. The V_B value decreased from 718.5 to 108.0 V/mm with increasing sintering temperature. The ZNR sintered at the range of 1240–1260 °C provide very high breakdown voltage (718.5–525.1 V/mm) above 500 V/mm per unit thickness of ceramics. Therefore, it is assumed that these ZNR could be applied as compact devices with high energy absorption capability. As the sintering temperature increased, the decrease of breakdown voltage is attributed firstly to the decrease in the number of grain boundaries caused by the increase of the ZnO grain size, and secondly, the abrupt decrease of v_{gb} value. The v_{gb} value was in the range of 2.8–3.0 V/gb for the ZNR sintered at 1240–1260 °C. However, the ZNR sintered at 1300 °C exhibited a much lower v_{gb} value, 0.9 V/gb than the general value of 2–3 V/gb. These ZNR exhibit very poor nonlinear properties. The v_{gb} is calculated by the following equation: $V_B = N_{gb} v_{gb} = (D/d) v_{gb}$, where N_{gb} is the number of grain boundaries, d is the average grain size, and D is the thickness of sample.

Fig. 6 shows the nonlinear coefficient (α) and leakage current (I_L) as a function of sintering temperature. As the

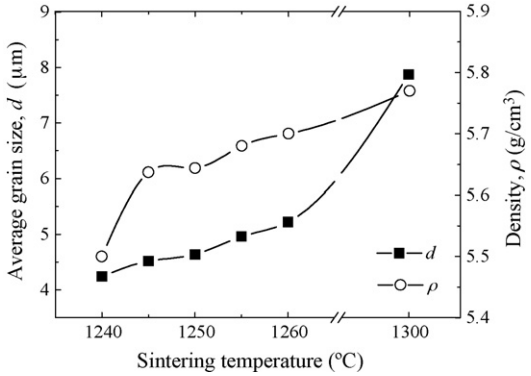

Fig. 3. Average grain size and sintered density as a function of sintering temperature.

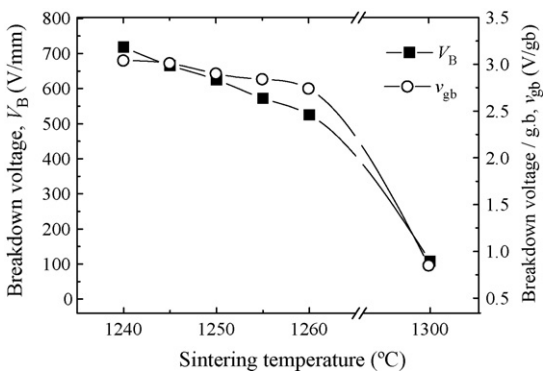

Fig. 5. Breakdown voltage and breakdown per grain boundary as a function of sintering temperature.

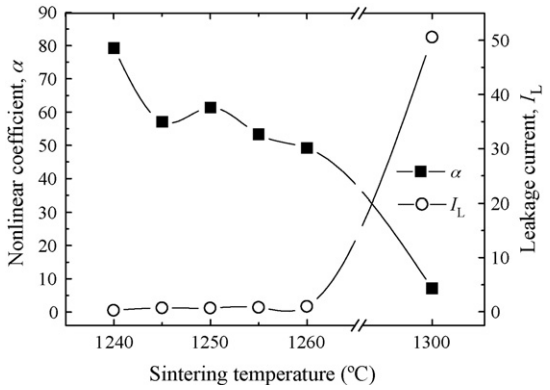

Fig. 6. Nonlinear coefficient and leakage current as a function of sintering temperature.

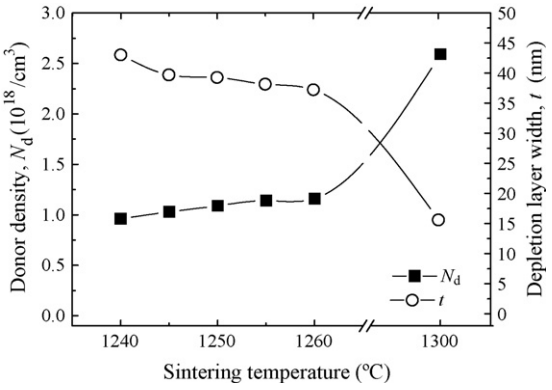

Fig. 8. Donor density and depletion layer width as a function of sintering temperature.

sintering temperature increased, the α value decreased from 79.3 to 7.1. The ZNR sintered at the range of 1240–1260 °C exhibited a high α value, above 50, whereas at 1300 °C, the α value was only 7.1. It is assumed that strong deterioration of nonlinear properties of the ZNR sintered at 1300 °C is attributed to excess segregation of La_2O_3, which presumably causes the electronic inactivity of grain boundaries; lowering potential barrier height at grain boundaries. This shows the sintering temperature greatly affects nonlinear properties. On the other hand, as the sintering temperature increased, the I_L value increased, achieving a minimum value 0.3 μA for the ZNR sintered at 1240 °C. Increasing sintering temperature further to 1300 °C caused the I_L value (50.6 μA) to increase greatly. Overall variation of I_L with sintering temperature showed the opposite variation to α. These variations of nonlinear properties with sintering temperature are closely related to the Schottky barrier at the grain boundary.

Fig. 7 shows the *C–V* characteristics of the ZNR at different sintering temperatures. The presence of Schottky barrier is inferred not only from nonlinearity of conduction but also from the voltage dependence of the capacitance. When DC bias is applied to ZNR, the capacitance decreases due to the increase of depletion layer width at active grain boundaries. The modified *C–V* equation is used to calculate various characteristic parameters. The *C–V* characteristic parameters include the donor density (N_d) of zinc oxide grain, density of interface states (N_t) at the grain boundary, barrier height (ϕ_b), and depletion layer width (t). The donor density (N_d) and depletion layer width (t) as a function of sintering temperature are shown in Fig. 8. The N_d value gradually increased from 0.96×10^{18} to 1.16×10^{18} cm^{-3} up to 1260 °C. However, the N_d value increased to 2.59×10^{18} cm^{-3} for sintering temperature of 1300 °C. The increase of N_d value is assumed to be due to the dissociation of zinc oxide in the following chemical reaction expression, $ZnO \rightarrow Zn_i^x + \frac{1}{2}O_2$, $Zn_i^x \rightarrow Zn_i^{\bullet} + e'$, where Zn_i^x is a neutral zinc of interstitial site, $Zn_i^{\bullet}$ is a positively charged zinc ion of interstitial site. It is assumed that the enhancement of the donor density gives rise to larger quantities of dissociation of zinc oxide when the sintering temperature increases. The t-value on either side of the depletion region decreased from 43.0 to 15.6 nm with increasing sintering temperature. This shows the opposite relation to N_d. In general, the depletion region extends farther into the side with a lighter doping.

Fig. 9 shows the density of interface states (N_t) and barrier height (ϕ_b) as a function of sintering temperature. As the sintering temperature increased between 1240 and 1255 °C, the N_t value increased from 4.13×10^{12} to 4.35×10^{12} cm^{-2}, whereas thereafter the N_t value decreased. The ϕ_b value decreased from 1.90 to 0.67 eV. In particular, it greatly decreased at 1300 °C. This coincides with the variation of α value in *V–I* characteristics. The ϕ_b is directly associated with the N_d and N_t. In other words, the ϕ_b is estimated by the

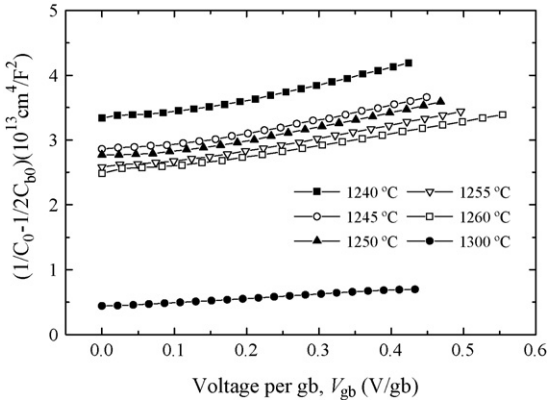

Fig. 7. *C–V* characteristics of the ZNR at different sintering temperatures.

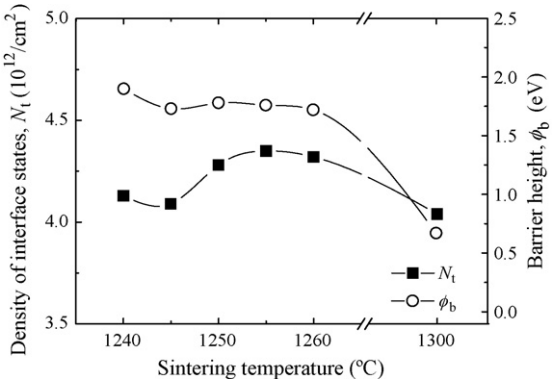

Fig. 9. Density of interface states and barrier height as a function of sintering temperature.

Table 1
Apparent dielectric constant and dissipation factor of the ZNR at different sintering temperatures

Sintering temperature (°C)	1240	1245	1250	1255	1260	1300
ε'_{APP}	411	475	496	546	583	2129
tan δ (%)	8.7	9.9	9.9	10.4	10.9	28.3

variation rate in the N_t and N_d. In general, the ϕ_b is increased with increasing N_t and decreasing N_d. If the variation rate of N_d is much larger than that of N_t with sintering temperature, the ϕ_b is much more strongly affected by the N_d than the N_t. According to this reason, it can be understood that the ϕ_b increases or decreases with increasing sintering temperature.

The dielectric parameters, including the apparent dielectric constant (ε'_{APP}) and dissipation factor (tan δ) are summarized in Table 1. As the sintering temperature increased up to 1260 °C, the ε'_{APP} value linearly gradually increased from 411 to 583 at 1 kHz, whereas it increased to 2129 at 1300 °C. This is directly related to the average grain size, as can be seen in the following equation, $\varepsilon'_{APP} = \varepsilon_g(d/t)$, where ε_g is the dielectric constant of ZnO (8.5), d is the average grain size, and t is the depletion layer width of the both sides at the grain boundaries. That is, this is because the increase of sintering temperature causes the decrease of total depletion layer width within entire bulk due to the increase of average grain size. On the other hand, as the sintering temperature increased to 1260 °C, the tan δ value linearly gradually increased from 8.7 to 10.9 at 1 kHz, whereas it increased up to 28.3 at 1300 °C. The variation of tan δ coincides with that of leakage current. The tan δ is composed of both frictional loss due to dipole rotation and Joule loss due to leakage current.

4. Conclusions

The microstructure, electrical properties, and dielectric characteristics of the ZNR doped with Pr–Co–Cr–La were investigated with different sintering temperatures of 1240, 1245, 1250, 1255, 1260, and 1300 °C. The ceramics more densified from 5.50 to 5.77 g/cm^3 with increasing sintering temperature. As the sintering temperature increased, it was found that the breakdown voltage decreases from 718.5 to 108.0 V/mm and the nonlinear coefficient decreases from 79.3 to 7.1.

The gap between sintering temperatures is small only 5 °C, however, it significantly affected electrical and dielectric characteristics in these ceramics. Conclusively, the ZNR sintered at 1240, 1245, 1250, 1255, and 1260 °C could be applied for high voltage with compact size because they provide high sintered density, high breakdown voltage, and high nonlinearity.

References

[1] L.M. Levinson, H.R. Pilipp, Zinc oxide varistor—a review, Am. Ceram. Soc. Bull. 65 (1986) 639–646.
[2] T.K. Gupta, Application of zinc oxide varistor, J. Am. Ceram. Soc. 73 (1990) 1817–1840.
[3] Y.-S. Lee, T.-Y. Tseng, Phase identification and electrical properties in ZnO-glass varistors, J. Am. Ceram. Soc. 75 (1992) 1636–1640.
[4] A.B. Alles, V.L. Burdick, The effect of liquid-phase sintering on the properties of Pr_6O_{11}-based ZnO varistors, J. Appl. Phys. 70 (1991) 6883–6890.
[5] A.B. Alles, R. Puskas, G. Callahan, V.L. Burdick, Compositional effect on the liquid-phase sintering of praseodymium oxides-based ZnO varistors, J. Am. Ceram. Soc. 76 (1993) 2098–2102.
[6] Y.-S. Lee, K.-S. Liao, T.-Y. Tseng, Microstructure and crystal phases of praseodymium in zinc oxides varistor ceramics, J. Am. Ceram. Soc. 79 (1996) 2379–2384.
[7] N. Wakiya, S.Y. Chun, C.H. Lee, O. Sakurai, K. Shinozaki, N. Mizutani, Effect of liquid phase and vaporization on the formation of microstructure of Pr doped ZnO varistor, J. Electroceram. 4:S1 (1999) 15–23.
[8] S.Y. Chun, N. Mizutani, Mass transport via grain boundary in Pr-based ZnO varistors and related electrical effects, Mater. Sci. Eng. B79 (2001) 1–5.
[9] C.-W. Nahm, The Electrical properties and d.c. degradation characteristics of Dy_2O_3 doped Pr_6O_{11}-based ZnO varistors, J. Eur. Ceram. Soc. 21 (2001) 545–553.
[10] C.-W. Nahm, C.-H. Park, Effect of Er_2O_3 addition on the microstructure, electrical properties, and stability of Pr_6O_{11}-based ZnO ceramic varistors, J. Mater. Sci. 36 (2001) 1671–1677.
[11] C.-W. Nahm, Electrical properties and stability against DC accelerated aging stress of ZPCCE-based varistor ceramics, J. Mater. Sci.: Mater. Electron. 15 (2004) 29–36.
[12] C.-W. Nahm, B.-C. Shin, B.-H. Min, Microstructure and electrical properties of Y_2O_3-doped ZnO–Pr_6O_{11}-based varistor ceramics, Mater. Chem. Phys. 82 (2003) 157–164.
[13] C.-W. Nahm, J.-A. Park, B.-C. Shin, I.-S. Kim, Electrical properties and DC accelerated aging behavior of ZnO–Pr_6O_{11}–CoO–Cr_2O_3–Dy_2O_3-based varistor ceramics, Ceram. Int. 30 (2005) 1009–1016.
[14] C.-W. Nahm, Effect of La_2O_3 addition on microstructure and electrical properties of ZnO–Pr_6O_{11}-based varistor ceramics, J. Mater. Sci.: Mater. Electron. 16 (2005) 345–349.
[15] J.C. Wurst, J.A. Nelson, Lineal intercept technique for measuring grain size in two-phase polycrystalline ceramics, J. Am. Ceram. Soc. 55 (1972) 109–111.
[16] M. Mukae, K. Tsuda, I. Nagasawa, Capacitance-vs-voltage characteristics of ZnO varistor, J. Appl. Phys. 50 (1979) 4475–4476.
[17] L. Hozer, Semiconductor Ceramics: Grain Boundary Effects, Ellis Horwood, London, 1999, 22.
[18] K. Mukae, Zinc oxide varistors with praseodymium oxide, Am. Ceram. Soc. Bull. 66 (1987) 1329–1331.